

Time-Resolved Measurement of X-Ray Heating in Plastic Foils Irradiated by Intense Soft-X-Ray Pulses

J. Edwards, M. Dunne, D. Riley, R. Taylor, and O. Willi

Blackett Laboratory, Imperial College of Science, Technology and Medicine, London SW7 2BZ, United Kingdom

S. J. Rose

Rutherford Appleton Laboratory, Chilton, Didcot, Oxon OX11 0QX, United Kingdom

(Received 13 August 1991)

Intense, soft-x-ray pulses, generated from separate laser-irradiated converters, were used to irradiate planar plastic foils. The x-ray heating was investigated by measuring the temperature histories of chlorinated tracer layers buried at different depths in the targets. The temperature diagnostic was a time-resolved extreme-UV absorption spectroscopy technique using chlorine *L*-shell transitions. The temporal temperature profiles were reasonably well reproduced by radiation-hydrocode simulations.

PACS numbers: 52.50.Jm, 44.40.+a, 52.25.Qt

With the use of modern high-power laser systems, it is now possible to generate intense, approximately Planckian x-ray sources. These are currently of considerable interest as possible driving power sources for indirect-drive inertial confinement fusion. In addition, they may be used for the production of uniform, gradient-free, hot, dense plasmas which cannot be produced by other means in the laboratory and which are ideal for the testing of theoretical calculations of, for example, opacities, radiative transfer, and dense plasma effects which are important for laboratory as well as astrophysical research. Therefore, an understanding of the interaction of intense, soft-x-ray pulses with targets is important for the design and interpretation of future experiments. In previous experimental work, x-ray preheating in laser-irradiated targets has been investigated [1,2]. However, few experimental studies using x-ray heating of plasmas alone have been reported. Evidence for ionization burnthrough of thin aluminum foils directly heated by x rays has been observed [3]. The opacity of a radiatively heated aluminum plasma, close to local thermodynamic equilibrium (LTE), has been measured in the region of the aluminum *K*-shell transitions [4] and evidence of radiation waves in gold foils has been observed [5]. Here we present the first measurements of x-ray heating as a function of time and depth in plastic foils irradiated by intense, approximately Planckian soft-x-ray pulses emitted from separate, laser-irradiated, high-*Z* converters. Plasma temperatures were measured with a novel, time-resolved, extreme-ultraviolet (XUV) absorption spectroscopy technique in the sub-keV photon energy region using *L*-shell transitions of chlorine ions present in thin tracer layers buried at different depths in the targets. Similar methods have been used to diagnose laser-irradiated targets using inner-shell transitions in the photon energy region above 1 keV [6,7]. It was found that the measured temperature profiles were reasonably well reproduced by radiation-hydrocode simulations.

Six frequency-doubled (0.53 μm wavelength) beams

from the VULCAN glass laser at the Rutherford Appleton Laboratory were used in a cluster configuration to irradiate a thin gold layer, 1000 \AA thick, supported on a 1- μm plastic (CH) substrate (hereafter the burnthrough or source target). Random-phase plates were used to produce a smoothed focal spot which was measured to be 500 μm (FWHM) in diameter by an x-ray pinhole camera filtered for photons in the 1-keV energy region. The laser pulse length was typically 800 ps in duration. The soft x rays transmitted through the rear of the burnthrough target were used to heat a separate planar CH foil, 2 μm thick, positioned parallel to the burnthrough foil and separated from it by approximately 250 μm . A thin chlorinated tracer layer ($\text{C}_8\text{H}_6\text{Cl}_2$), 0.3 μm thick, was buried at different depths in the CH foils. The soft x rays transmitted through the target were analyzed using time-resolved, flat-field, XUV spectroscopy in the 50- \AA spectral wavelength region [8]. The temporal and spectral resolutions were approximately 50 ps and 0.3 \AA , respectively. The spectral region was calibrated with emission lines from a carbon plasma and with the carbon *K*-shell photoabsorption edge produced by a cold filter. A pair of parallel, highly polished fused silica mirrors were used in front of the spectrometer to act as a cutoff filter for x rays with energies above about 600 eV to reduce multiple-order effects.

The experimental conditions have been simulated with a multigroup radiation transport model coupled to the 1D Lagrangian hydrodynamics code MEDUSA [9]. The radiation transport code uses 116 groups in the 0-100-keV energy region. Group-averaged Planck mean opacities are used and are calculated in-line with the hydrodynamics assuming LTE from a screened-hydrogenic, average-atom (AA) model similar to XSN [10]. The assumption of LTE was assessed using a non-LTE AA model to calculate the average atomic level populations for the predicted plasma conditions. It was found that LTE was a good approximation during most of the simulations. In the calculations, a CH foil was heated with an x-ray pulse

whose temporal behavior was that measured experimentally from the rear of a burnthrough foil when no sample target was present for similar experimental conditions. At the peak of the x-ray pulse, the spectrum was assumed to be Planckian. The introduction of additional spectral features to simulate *M*-, *N*-, and *O*-shell emission was found to have little effect on the results. The x-ray conversion efficiency from the burnthrough target was estimated from time-resolved and time-integrated XUV photodiode measurements taken under similar experimental conditions when a value of $(5.5 \pm 2)\%$ was found [11]. The value used in the 1D simulations was adjusted to give the best agreement with the experimental measurements to account for the geometrical coupling of the source emission to the target and variations in the conversion efficiency. MEDUSA uses a Thomas-Fermi equation of state (EOS) to describe the electrons with corrections to give correct solid density, while the ions are described by a perfect-gas EOS. Energy transfer by thermal electrons is calculated using flux-limited conduction. Simulations performed both with and without thermal electron conduction included in the calculation showed no noticeable differences in the predictions.

Detailed spectral analysis of the experimental results has been performed using a spectral analysis package (SAP) containing an extensive atomic database (oscillator strengths, level, and transitions energies) generated by a multiconfiguration Dirac-Fock (MCDF) atomic physics code [12]. In the calculation of the transition energies, the initial and final atomic states are optimized separately [13]. Ionic distributions are calculated with the Saha equation (i.e., assuming LTE). The line shape is taken to be Lorentzian with a width given by an approximate expression [14]. Bound-free cross sections have not been included for chlorine but this is not expected to affect the results. Synthetic absorption spectra are generated from the calculated opacities by solving the time-independent equation of transfer in one dimension for a given plasma density, temperature, and thickness. The predicted spectrum is convolved with the instrumental function, in this case taken to be a Gaussian with a FWHM given by the instrument resolution. Plasma conditions are inferred by comparing the predicted spectra with those observed experimentally. Calculations were performed for the tracer

layer only. The remainder of the target introduces no discontinuous absorption features in the energy range of interest and only affects the slope of the underlying continuum as verified when targets with no tracer layers were used. The analysis is based mainly on *2p-3d* transitions of F-like to S-like chlorine ions. For Al-like to S-like ions, some of the relevant transition data could not be calculated with MCDF. This affects the analysis at early time only ($t \leq 300\text{--}500$ ps). A detailed description of SAP will be presented elsewhere together with a list of all the bound-bound transitions.

Figure 1 shows a comparison between streaked spectra obtained from targets with the $0.3\text{-}\mu\text{m}$ tracer layer buried $0.2\ \mu\text{m}$ (left) and $1.8\ \mu\text{m}$ (right) below the surface of a $2\text{-}\mu\text{m}$ CH target. The laser irradiance in these cases was $2 \times 10^{14}\ \text{W cm}^{-2}$. Assuming a 5% conversion efficiency, this corresponds to an x-ray flux of approximately $(2\text{--}5) \times 10^{12}\ \text{W cm}^{-2}$ at the sample. The positions of some *2p-3d* transitions of F-like to Na-like chlorine are marked. The broad band of absorption observed at early time is due to *2p-3d* transitions in chlorine ions with a partially filled *M* shell. The sharp fall in the signal below a wavelength of around $43\ \text{\AA}$ is due largely to absorption by a combination of the instrumental filters and the remainder of the target foil.

Several distinct differences between the two spectra can be observed. When the chlorinated layer is placed $0.2\ \mu\text{m}$ below the front surface of the target (front layer), the band of *2p-3d* transitions shifts towards shorter wavelength (higher energy) more rapidly than when the layer is positioned at a depth of $1.8\ \mu\text{m}$ (rear layer), indicating a more rapid ionization of the material in the front layer. This can also be seen from the earlier turn-on of Na-like and Ne-like absorption features (by $\sim 200\text{--}300$ ps) in the spectrum from the front layer. In addition, the chlorine becomes more highly ionized in the front layer indicating that a higher temperature is attained here. This can be seen from the appearance of F-like absorption features approximately 500 ps after the start of the x-ray pulse. In contrast, little evidence is seen for the presence of significant fractions of F-like ions in the rear layer. Also, the *2p-3d* Na-like absorption feature remains prominent for the layer at the rear of the target whereas it becomes almost unnoticeable after about 900 ps when the layer is positioned near the front surface.

The temperature histories of the tracer layers were inferred as a function of time by comparing the experimental data with detailed, synthetic, absorption spectra calculated by SAP. Calculations were performed for temperatures between 5 and 50 eV at 5-eV intervals and for densities between 1 and $0.005\ \text{g/cm}^3$ with a ratio between successive values of approximately 2. Figure 2 shows a comparison between a densitometer trace taken approximately 900 ps after the start of the emission from the front layer spectrum shown in Fig. 1 and an absorption spectrum calculated with SAP for a density of $0.02\ \text{g/cm}^3$ and a temperature of 40 eV. For comparison, a trace

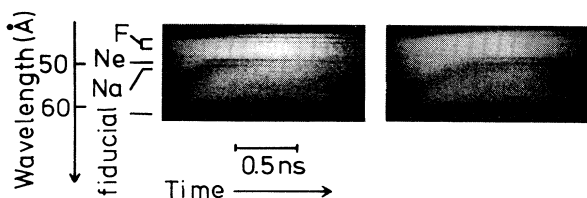


FIG. 1. Streaked spectra taken from $2\text{-}\mu\text{m}$ plastic targets with chlorinated tracer layers buried $0.2\ \mu\text{m}$ (left) and $1.8\ \mu\text{m}$ (right) below the surface. Some *2p-3d* transitions of F-, Ne-, and Na-like chlorine are marked.

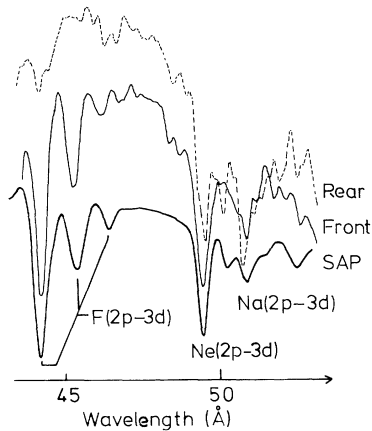


FIG. 2. Traces taken across spectra from Fig. 1 near the peak of the emission and a spectrum predicted by SAP for 40 eV and 0.02 g/cm^3 . Some $2p-3d$ transitions are marked. For clarity the spectra have been displaced vertically.

taken across the spectrum produced by the chlorinated layer positioned near the rear of a plastic target is also shown. The density is taken from the hydrocode simulation and the temperature has been chosen to give best agreement between the experimentally measured and synthetic spectra. Figure 3 shows a comparison between the temperature histories inferred from the absorption spectra shown in Fig. 1 and those predicted by the radiation hydrocode using a “best-fit” x-ray conversion efficiency of 2.5%. The solid curves show the range of temperatures predicted by the hydrocode to exist in the tracer layers while the vertical bars show the experimental measurements. The uncertainty in the inferred temperature histories arising from taking the layer densities to be those predicted by the hydrocode has been estimated by assuming a density error of approximately a factor of 2 when comparing the experimental and synthetic spectra. This leads to approximately 10% uncertainty in the inferred temperatures. The additional error resulting from variations in the predicted density profiles due to up to a factor-of-2 change in the x-ray conversion efficiency has also been included but is substantially less than the 10% resulting from the factor-of-2 assumed density error of the hydrocode. The vertical error bars on the experimental points also include the estimated uncertainty in the inferred temperature both due to the discrete density and temperature values at which the synthetic spectra were calculated and due to spatial gradients in the layers parallel and perpendicular to the target surface. Therefore, the error bars are not necessarily the same at each time. It is estimated that the uncertainty in the relative timings of the experimental and predicted curves is approximately 100 ps. The onset of the gold emission at around 45 \AA is taken to be the beginning of the x-ray heating pulse. This is because most of the x-ray pulse energy exists in this spectral region and because the sample

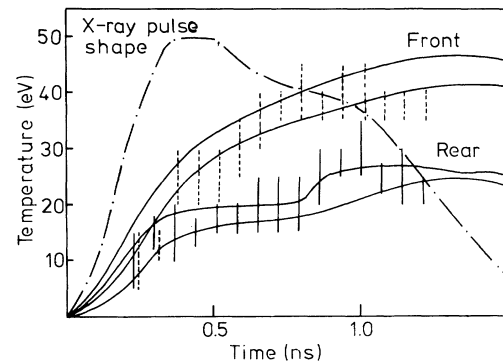


FIG. 3. Comparison of experimentally measured temperature histories inferred from the spectra of Fig. 1 and those predicted by the radiation hydrocode. The x-ray pulse shape is shown.

target is no more than approximately one photon-mean-free-path thick in this photon energy region so that the measurement of the start of the x-ray pulse is not significantly affected by the presence of the sample foil. For reference, the x-ray pulse shape is also shown.

The overall agreement between the experimentally measured points and the hydrocode simulations is reasonably good. In particular, the different shapes of the temporal profiles for the front and rear layers are reproduced well. In the simulations, the rear layer is “preheated” (0–400 ps) to temperatures above that of the ambient CH by radiation mainly in the “carbon window” below the K edge where the intervening CH is optically thin. A significant fraction of the x rays in this region are absorbed in the chlorinated layer due to bound-free chlorine L -shell transitions. As the layer heats and ionizes, its opacity in the carbon window region decreases as the chlorine L -shell bound-free threshold shifts towards higher energy. As a result, the layer heating rate is reduced and a temperature plateau is established (400–800 ps). The intervening CH is heated mainly by x rays in the energy regions just above and well below the carbon K edge where the photon mean free path is submicron. As the material is ionized, the opacity is reduced and, in particular in this case, the K edge shifts towards higher energy allowing radiation in this region (a significant fraction of the source spectrum) to propagate into the cooler material where it is strongly absorbed. It is the propagation of this “ionization front” that is responsible for the step in the simulated rear layer profile at around 850 ps. Bound-free threshold shifting has been identified as being responsible for enhanced radiation transport into the cooler material away from the ablation region in laser-target simulations [15]. This type of behavior may also be responsible for the shape of the experimentally measured rear layer temperature history. Similar behavior is not predicted for the front layer because the $0.2 \mu\text{m}$

of intervening CH is optically thin to the source over most of the photon energy spectrum and therefore will have little effect on the layer heating.

In conclusion, an experiment has been performed to investigate the x-ray heating in plastic foils irradiated by intense, approximately Planckian x-ray pulses, generated by separate, laser-irradiated, high- Z converters. The temperature histories of chlorinated tracer layers buried at different depths in the targets were measured with a novel, time-resolved, XUV, absorption spectroscopy technique utilizing L -shell transitions of chlorine ions. The temporal temperature profiles were reproduced well by radiation hydrocode simulations and the form of the rear layer profile may result from the propagation of an ionization front in the plastic foil.

During this work, we have become indebted to many people including the following: the staff of the Central Laser Facility for their considerable support and effort during the experiment; C. Back who was involved in a previous experiment to measure soft-x-ray conversion efficiencies from the burnthrough targets; and employees of AWE, in particular J. Foster, for the loan of a high-time-resolution flat-response x-ray detector for x-ray conversion measurements. This work was funded jointly by the SERC and MoD.

[1] E. A. McLean *et al.*, Phys. Rev. Lett. **45**, 1246 (1989); S. H. Gold and E. A. McLean, J. Appl. Phys. **53**, 784

- (1982).
- [2] A. Ng, D. Parfeniuk, L. DaSilva, and D. Pasini, Phys. Fluids **28**, 2915 (1985).
- [3] T. Mochizuki *et al.*, Phys. Rev. A **36**, 3279 (1987).
- [4] S. J. Davidson, J. M. Foster, S. J. Rose, C. C. Smith, and K. A. Warburton, Appl. Phys. Lett. **52**, 847 (1988).
- [5] R. Sigel *et al.*, Phys. Rev. Lett. **65**, 587 (1990).
- [6] A. Hauer *et al.*, Phys. Rev. A **34**, 411 (1986).
- [7] C. Chenais-Popovics *et al.*, Phys. Rev. A **40**, 3194 (1989).
- [8] G. Kiehn, T. Garvey, R. Smith, O. Willi, A. Damerell, and J. West, Proc. SPIE Int. Soc. Opt. Eng. **831**, 150 (1987).
- [9] J. P. Christiansen, D. E. T. F. Ashby, and K. V. Roberts, Comput. Phys. Commun. **7**, 271 (1974); P. A. Rodgers, A. M. Rogoyski, and S. J. Rose, MED101: a laser-plasma simulation code. User guide (Rutherford Appleton Laboratory Report No. RAL-89-127, 1989).
- [10] W. A. Lokke and W. H. Grasberger, Lawrence Livermore National Laboratory Report No. UCRL-52276, 1977 (unpublished).
- [11] J. Edwards *et al.*, in Proceedings of the Sarasota Workshop on the Properties of Hot Dense Matter (World Scientific, Singapore, to be published).
- [12] I. P. Grant, B. J. McKenzie, P. H. Norrington, D. F. Mayers, and N. C. Pyper, Comput. Phys. Commun. **21**, 207 (1980); B. J. McKenzie, I. P. Grant, and P. H. Norrington, Comput. Phys. Commun. **21**, 233 (1980).
- [13] S. J. Rose, J. Quant. Spectrosc. Radiat. Transfer **36**, 389 (1986).
- [14] E. Nardi and Z. Zinamon, Phys. Rev. A **20**, 1197 (1979).
- [15] D. Duston, R. W. Clark, and J. Davis, Phys. Rev. A **31**, 3220 (1985).

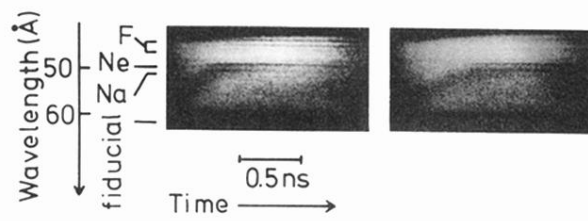


FIG. 1. Streaked spectra taken from 2- μm plastic targets with chlorinated tracer layers buried 0.2 μm (left) and 1.8 μm (right) below the surface. Some $2p$ - $3d$ transitions of F-, Ne-, and Na-like chlorine are marked.